Entropy **2015**, *17*, 5980-5994; doi:10.3390/e17095980

OPEN ACCESS

entropy

ISSN 1099-4300

www.mdpi.com/journal/entropy

Article

Numerical Investigation into Natural Convection and Entropy Generation in a Nanofluid-Filled U-Shaped Cavity

Ching-Chang Cho [1], Her-Terng Yau [2,*], Ching-Huang Chiu [1] and Kuo-Ching Chiu [1]

[1] Department of Vehicle Engineering, National Formosa University, No.64, Wunhua Rd., Huwei Township, Yunlin County 63201, Taiwan; E-Mails: cccho@nfu.edu.tw (C.-C.C.); chc@sunws.nfu.edu.tw (C.-H.C.); joo@sunws.nfu.edu.tw (K.-C.C.)

[2] Department of Electrical Engineering, National Chin-Yi University of Technology, 35, 215 Lane, Sec. 1, Chung Shan Road, Taiping, Taichung City 41170, Taiwan

* Author to whom correspondence should be addressed; E-Mail: htyau@ncut.edu.tw; Tel.: +886-04-2392-4505 (ext. 7229); Fax: +886-04-2393-0062.

Academic Editor: Kevin H. Knuth

Received: 4 July 2015 / Accepted: 25 August 2015 / Published: 26 August 2015

Abstract: This current work studies the heat transfer performance and entropy generation of natural convection in a nanofluid-filled U-shaped cavity. The flow behavior and heat transfer performance in the cavity are governed using the continuity equation, momentum equations, energy equation and Boussinesq approximation, and are solved numerically using the finite-volume method and SIMPLE C algorithm. The simulations examine the effects of the nanoparticle volume fraction, Rayleigh number and the geometry parameters of the U-shaped cavity on the mean Nusselt number and total entropy generation. It shows that the mean Nusselt number increases and the total entropy generation reduces as the volume fraction of nanoparticles increases. In addition, the results show that the mean Nusselt number and the total entropy generation are both increased as the Rayleigh number increases. Finally, it also shows that mean Nusselt number can be increased and the total entropy generation can be reduced by extending the length of the low temperature walls or widening the width of the low temperature walls.

Keywords: entropy generation; nanofluid; heat transfer enhancement; cavity; natural convection

1. Introduction

During all fluid flow and heat transfer processes, useful energy will be lost due to the generation of irreversibilities. Generally, the magnitude of these irreversibilities can be estimated by the rate of the entropy generation. Therefore, in a system, it is necessary to minimize the rate of the entropy generation so that the useful energy can be maximized [1,2].

Natural convection in cavities is of great practical interest in many engineering applications, including electronic cooling devices, heat exchangers, electric machinery, solar energy collectors, and so on [3]. To optimize the useful energy in such applications, many researchers have studied the entropy generation of natural convection in cavities. For example, Erbay *et al*. [4,5] and Magherbi *et al*. [6] studied the transient entropy generation of natural convection in square cavities with completely- or partially-heated left-side walls, respectively, and a completely cooled right-side wall. They have considered the effects of heat transfer irreversibility and fluid friction irreversibility on the entropy generation and had analyzed the transient behavior of the entropy generation in the studied cavity. Bounabid *et al.* [7] analyzed the transient entropy generation of natural convection in an inclined rectangular cavity comprising vertical isothermal walls and adiabatic horizontal walls. Their results have shown that the entropy generation increased with the increases of Grashof number, irreversibility distribution ratio and aspect ratio of the cavity. Ilis *et al*. [8] investigated the entropy generation caused by natural convection in a rectangular cavity with a high-temperature left-side wall and a low-temperature right-side wall. Their results have indicated that depending on the Rayleigh number and irreversibility distribution ratio, the total entropy generation of the cavity was dominated by the heat transfer irreversibility or by the fluid friction irreversibility. Mukhopadhyay [9] examined the entropy generation induced by natural convection in a square cavity heated by two isoflux sources. Their results have shown that the entropy generation can be optimized by turning the length and position of the heat sources. Dagtekin *et al*. [10] analyzed the entropy generation of natural convection in a Γ-shaped cavity with a heated step. Their results showed that at low Rayleigh numbers, the effect of the aspect ratio on the entropy generation in the studied cavity was not significant and the entropy generation was dominated mainly by the heat transfer irreversibility. However, at high Rayleigh numbers, the effect of the aspect ratio on the entropy generation was significant and the effect of the fluid friction irreversibility on the entropy generation becomes more effective.

Nanofluids consist of nanoparticles with high thermal conductivity suspended in a base fluid with low thermal conductivity [11]. As a result, nanofluids provide excellent thermophysical properties than conventional working fluids. Recently, many researchers have studied the entropy generation of natural convection in nanofluid-filled cavities. For example, Shahi *et al*. [12] studied the entropy generation of natural convection in a nanofluid-filled square cavity heated by a protruding heat source. Their results have shown that the entropy generation reduced as the nanoparticle volume fraction was increased. In addition, their results have also shown that the entropy generation could be minimized when the heat source was positioned on the lower wall of the cavity. Kefayati [13] presented a numerical investigation into the entropy generation due to natural convection in a non-Newtonian nanofluid-filled cavity bounded by two isothermal vertical walls and two adiabatic horizontal walls. Their results showed that the Bejan number reduced as the Rayleigh number increased. In addition, their results also showed that the addition of nanoparticles caused a decrease in the Bejan number. Parvin and Chamkha [14] examined the entropy generation of natural convection in an odd-shaped cavity filled with Cu–water nanofluid.

The results showed that in the odd-shaped cavity, the entropy generation could be minimized by giving a particular Rayleigh number. Cho *et al*. [15] investigated the entropy generation induced by natural convection in a water-based nanofluid-filled cavity bounded by a left wavy-wall with a constant heat flux, a right wavy-wall with a constant low temperature, and flat upper and lower walls with adiabatic conditions. Their results showed that the entropy generation could by minimized via an appropriate tuning of the wavy surface geometry parameters. Cho [16] also investigated the entropy generation in a partially-heated wavy-wall square cavity filled with Al_2O_3-water nanofluid. The results have shown that in the studied cavity, the total entropy generation increased as the amplitude and wavelength of the wavy-surface increased. In addition, the results have also shown that given a suitable location of the partially-heated wavy surface in the cavity, the entropy generation could be reduced.

The natural convection heat transfer performance in a U-shaped cavity has been investigated [17]. However, the study of the entropy generation in a U-shaped cavity caused by natural convection is not presented in the literature. Therefore, the present work investigates the heat transfer performance and entropy generation of natural convection in a U-shaped cavity filled with Al_2O_3-water nanofluid. In performing the study, the flow behavior and heat transfer characteristics in the cavity are governed by the continuity equation, momentum equations, energy equation and Boussinesq approximation. Finite-volume method and SIMPLE C (semi-implicit method for pressure-linked equations consistent) algorithm are used to solve the governing equations numerically. The simulations focus specifically on the effects of the nanoparticle volume fraction, Rayleigh number, and geometry parameters of the U-shaped cavity on the mean Nusselt number and total entropy generation.

2. Mathematical Formulation

2.1. Governing Equations and Boundary Conditions

Figure 1 illustrates the U-shaped cavity considered in the present study. As shown, the cavity has a width W and a height H. The gravitational force (g) is assumed to act in the negative y-direction. It is assumed that the left and right walls of the cavity are heated by a constant heat flux (q_0''), and the concaves of the cavity are maintained at a constant low temperature (T_L). In addition, the other walls are assumed to be insulated. Meanwhile, a no-slip impermeable velocity boundary condition is used at all of the wall surfaces.

It is Assumed that the base fluid and nanoparticles are in thermal equilibrium, and no relative motion occurs between them; the nanoparticles have a uniform size and shape, and are well dispersed within the base fluid; that the thermophysical properties of the nanofluid are all constant, other than the density, which varies in accordance with the Boussinesq approximation; that the nanofluid within the cavity is Newtonian, incompressible and laminar; and the flow field is two-dimensional and in a steady state. Let the following non-dimensional quantities be introduced:

$$x^* = x/W,\ y^* = y/W,\ u^* = \frac{u}{\alpha_{bf}/W},\ v^* = \frac{v}{\alpha_{bf}/W},\ p^* = \frac{p}{\rho_{bf}\alpha_{bf}^2/W^2},\ \theta = \frac{T-T_L}{(q_0''W)/k_{bf}} \quad (1)$$

where u and v are the velocity components, α is the thermal diffusivity, p is the pressure, ρ is the density, θ is the dimensionless temperature, T is the temperature, T_L is the low temperature, k is the thermal conductivity, and subscript bf indicate the base fluid.

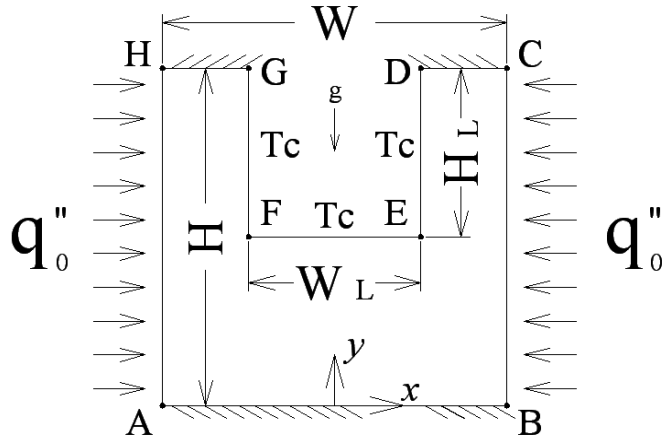

Figure 1. Schematic illustration of the U-shaped cavity. Note that g indicates the gravitational acceleration force; W and H are the width and height of the U-shaped cavity, respectively; and W_L and H_L are the width and height of the concave in the U-shaped cavity, respectively.

Under the assumption of ignoring the thermal radiation and viscous dissipation effects, the continuity equation, momentum equations and energy equation can be written in the following, non-dimensionalized forms:

$$\frac{\partial u^*}{\partial x^*}+\frac{\partial v^*}{\partial y^*}=0 \tag{2}$$

$$u^*\frac{\partial u^*}{\partial x^*}+v^*\frac{\partial u^*}{\partial y^*}=-\frac{\rho_{bf}}{\rho_{nf}}\frac{\partial p^*}{\partial x^*}+\frac{\nu_{nf}}{\nu_{bf}}\Pr\left(\frac{\partial^2 u^*}{\partial x^{*2}}+\frac{\partial^2 u^*}{\partial y^{*2}}\right) \tag{3}$$

$$u^*\frac{\partial v^*}{\partial x^*}+v^*\frac{\partial v^*}{\partial y^*}=-\frac{\rho_{bf}}{\rho_{nf}}\frac{\partial p^*}{\partial y^*}+\frac{\nu_{nf}}{\nu_{bf}}\Pr\left(\frac{\partial^2 v^*}{\partial x^{*2}}+\frac{\partial^2 v^*}{\partial y^{*2}}\right)+Ra\cdot\Pr\frac{(1-\varphi)(\rho\beta)_{bf}+\varphi(\rho\beta)_p}{\rho_{nf}\beta_{bf}}\theta \tag{4}$$

$$u^*\frac{\partial \theta}{\partial x^*}+v^*\frac{\partial \theta}{\partial y^*}=\frac{\alpha_{nf}}{\alpha_{bf}}\left(\frac{\partial^2 \theta}{\partial x^{*2}}+\frac{\partial^2 \theta}{\partial y^{*2}}\right) \tag{5}$$

where subscript nf and p indicate the nanofluid and nanoparticle, respectively; ν is the kinematic viscosity; φ is the volume fraction of nanoparticles in the base fluid; and β is the thermal expansion coefficient. In addition, Ra and Pr in Equations (3) and (4) are the Rayleigh number and Prandtl number, respectively, and are defined as

$$Ra=\frac{g\beta_{bf}W^3(q_0''W)/k_{bf}}{\nu_{bf}\alpha_{bf}} \tag{6}$$

$$\mathrm{Pr} = \frac{\nu_{bf}}{\alpha_{bf}} \tag{7}$$

The effective properties of the nanofluids given in Equations (2)–(5) can be estimated as follows [18–20]:

$$\rho_{nf} = (1-\varphi)\rho_{bf} + \varphi\rho_p \tag{8}$$

$$(\rho C_p)_{nf} = (1-\varphi)(\rho C_p)_{bf} + \varphi(\rho C_p)_p \tag{9}$$

$$\mu_{nf} = \frac{\mu_{bf}}{(1-\varphi)^{2.5}} \tag{10}$$

$$\frac{k_{nf}}{k_{bf}} = \frac{(k_p + 2k_{bf}) - 2\varphi(k_{bf} - k_p)}{(k_p + 2k_{bf}) + \varphi(k_{bf} - k_p)} \tag{11}$$

$$\alpha_{nf} = \frac{k_{nf}}{(\rho C_p)_{nf}} \tag{12}$$

Finally, the dimensionless boundary conditions can be written as follows:

$$\vec{V}^* = 0,\ \frac{\partial\theta}{\partial\vec{n}^*} = \frac{k_{bf}}{k_{nf}},\ \text{for } \overline{BC}, \overline{HA} \tag{13a}$$

$$\vec{V}^* = 0,\ \theta = 0,\ \text{for } \overline{DE}, \overline{EF}, \overline{FG} \tag{13b}$$

$$\vec{V}^* = 0,\ \frac{\partial\theta}{\partial\vec{n}^*} = 0,\ \text{for } \overline{AB}, \overline{CD}, \overline{GH} \tag{13c}$$

where $\vec{n}^*$ is the normal vector.

2.2. Nusselt Number

The Nusselt number (Nu) can be used to estimate the heat transfer performance. It is defined as follows:

$$Nu = \frac{hW}{k_{bf}} \tag{14}$$

where $h(= q_0'' / (T_s - T))$ is the convection heat transfer coefficient, and T_s is the surface temperature. The Nusselt number can be written in a non-dimensional form via substituting Equation (1) into Equation (14), *i.e.*,

$$Nu = \frac{1}{\theta_s} \tag{15}$$

The mean Nusselt number can be obtained as

$$Nu_m = \int_A^H Nu\,dy + \int_B^C Nu\,dy \tag{16}$$

2.3. Entropy Generation

The local entropy generation in a 2D cavity can be quantified as follows [1,2,15,16]:

$$\begin{aligned} S_l &= \frac{k_{nf}}{T^2}[(\frac{\partial T}{\partial x})^2+(\frac{\partial T}{\partial y})^2]+\frac{\mu_{nf}}{T}\{2[\left(\frac{\partial u}{\partial x}\right)^2+\left(\frac{\partial v}{\partial y}\right)^2]+\left(\frac{\partial u}{\partial y}+\frac{\partial v}{\partial x}\right)^2\} \\ &= S_{l,h}+S_{l,f} \end{aligned} \tag{17}$$

Note that $S_{l,h}(=\frac{k_{nf}}{T^2}[(\frac{\partial T}{\partial x})^2+(\frac{\partial T}{\partial y})^2])$ represents the local entropy generation due to heat transfer irreversibility, while $S_{l,f}(=\frac{\mu_{nf}}{T}\{2[\left(\frac{\partial u}{\partial x}\right)^2+\left(\frac{\partial v}{\partial y}\right)^2]+\left(\frac{\partial u}{\partial y}+\frac{\partial v}{\partial x}\right)^2\})$ represents the local entropy generation due to fluid friction irreversibility. Substituting Equation (1) into Equation (17), the local entropy generation can be written in the following non-dimensional form:

$$\begin{aligned} S_l^* &= \frac{k_{nf}}{k_{bf}}\cdot\frac{1}{(\theta+T_r)^2}[(\frac{\partial\theta}{\partial x})^2+(\frac{\partial\theta}{\partial y})^2]+\frac{Ec\cdot\mathrm{Pr}}{\theta+T_r}\cdot\frac{\mu_{nf}}{\mu_{bf}}\{2[(\frac{\partial u^*}{\partial x^*})^2+(\frac{\partial v^*}{\partial y^*})^2]+(\frac{\partial u^*}{\partial y^*}+\frac{\partial v^*}{\partial x^*})^2\} \\ &= S_{l,h}^*+S_{l,f}^* \end{aligned} \tag{18}$$

where $S_l^*(=\frac{W^2}{k_{bf}}S_l)$ is the non-dimensional local entropy generation, $Ec(=C_1/Ra)$ is the Eckert number, and T_r is equal to $T_r=C_2/Ra$. Note that C_1 and C_2 are constants with values of $C_1=\frac{\alpha_{bf}\beta_{bf}gW}{C_{p,bf}\nu_{bf}}$ and $C_2=\frac{\beta_{bf}gW^3T_L}{\alpha_{bf}\nu_{bf}}$, respectively. The total non-dimensional entropy generation is obtained as

$$S=\int S_l^* d\forall^* \tag{19}$$

where $\forall$ is the volume of the cavity.

In addition, the Bejan number (Be) is defined as follows:

$$Be=\frac{S_{l,h}^*}{S_l^*} \tag{20}$$

According to Equation (20), heat transfer irreversibility dominates the total entropy generation when $Be>0.5$, whereas fluid friction irreversibility dominates when $Be<0.5$. For the particular case of $Be=0.5$, the total energy generation is determined equally by the heat transfer irreversibility effect and the fluid friction irreversibility effect.

2.4. Numerical Solution Procedure and Numerical Validation

The governing equations and boundary conditions were discretized using the finite-volume numerical method [21]. The convection terms in the governing equations were discretized using the second-order upwind scheme. The velocity-pressure fields were coupled using the SIMPLE C algorithm [21]. The discretized algebraic equations were solved iteratively using a line-by-line TDMA (tri-diagonal matrix algorithm) scheme.

To validate the solution procedure, the numerical results obtained for the variation of the mean Nusselt number with the Rayleigh number in an air-filled square cavity were compared with [22,23]. It is shown in Table 1 that the present results are in good agreement with those presented in [22,23].

Table 1. Comparison of present results for mean Nusselt number with published results.

	$Ra = 10^3$	$Ra = 10^4$	$Ra = 10^5$	$Ra = 10^6$
Present results	1.118	2.247	4.537	8.931
De Vahl Davis [22]	1.118	2.243	4.519	8.799
Wan *et al*. [23]	1.117	2.254	4.598	8.976

3. Results and Discussion

In this study, Al_2O_3-water nanofluid is used to be the medium of thermal transportation. The thermophysical properties of the Al_2O_3 nanoparticles are given as follows [18]: specific heat, $C_p = 765\ J/kgK$; density, $\rho = 3970\ kg/m^3$; thermal conductivity, $k = 40\ W/mK$; and thermal expansion coefficient, $\beta = 0.85\times10^{-5}\ K^{-1}$. In addition, the thermophysical properties of the water are specified as follows: specific heat, $C_p = 4179\ J/kgK$; density, $\rho = 997.1\ kg/m^3$; thermal conductivity, $k = 0.613\ W/mK$; and thermal expansion coefficient, $\beta = 21\times10^{-5}\ K^{-1}$. In addition, the Prandtl number is given as $\mathrm{Pr} = 6.2$. Finally, it is assumed that the width of the cavity is equal to the height of the cavity, *i.e.*, $W = H$.

Prior to the simulations, a grid-independence analysis was performed to determine the mesh size. Figure 2 plots the variation of the mean Nusselt number with the grid size. It is seen that a grid size of 0.005×0.005 ensures a grid-independent solution. The computational domain was thus meshed accordingly.

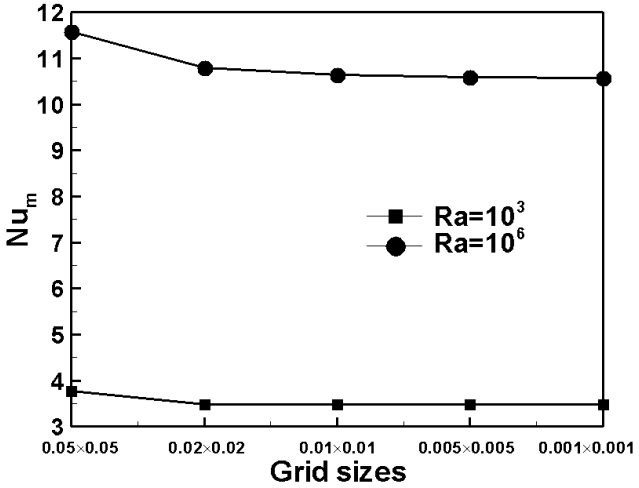

Figure 2. Variation of mean Nusselt number with grid mesh size. Note that $\varphi = 4\%$, $W_L = 0.3W$ and $H_L = 0.3W$.

Figure 3a–c show the flow streamlines, isotherms and entropy generation, respectively, within the U-shaped cavity for a Rayleigh number of $Ra = 10^3$ and different nanoparticle volume fractions. Figure 4a–c present the equivalent results for a Rayleigh number of $Ra = 10^6$. Since the U-shaped cavity is

heated by the left and right walls and is cooled by the concave walls of the U-shaped cavity, the fluid rises from the left and right walls and then falls along the concave walls of the U-shaped cavity. As a result, two flow circulation structures with opposite rotating direction are presented in the cavity (see Figures 3a and 4a). Given a low Rayleigh number, since the thermally-induced buoyancy effect is weak, the conduction mechanism dominates the heat transfer effect. Therefore, the strength of the flow streamlines is low (see Figure 3a) and the isotherms have no significantly twisting occurrence (see Figure 3b). Given a high Rayleigh number, since the thermally-induced buoyancy effect is strong, the convection mechanism dominates the heat transfer effect. As a result, the strength of the flow streamlines is high (see Figure 4a) and thus a significant twisting of the isotherms occurs (see Figure 4b). It is observed that the isotherms are concentrated near the heated and cooled walls. These regions experience a high temperature gradient, resulting in the formation of active regions for local entropy generation (see Figures 3c and 4c).

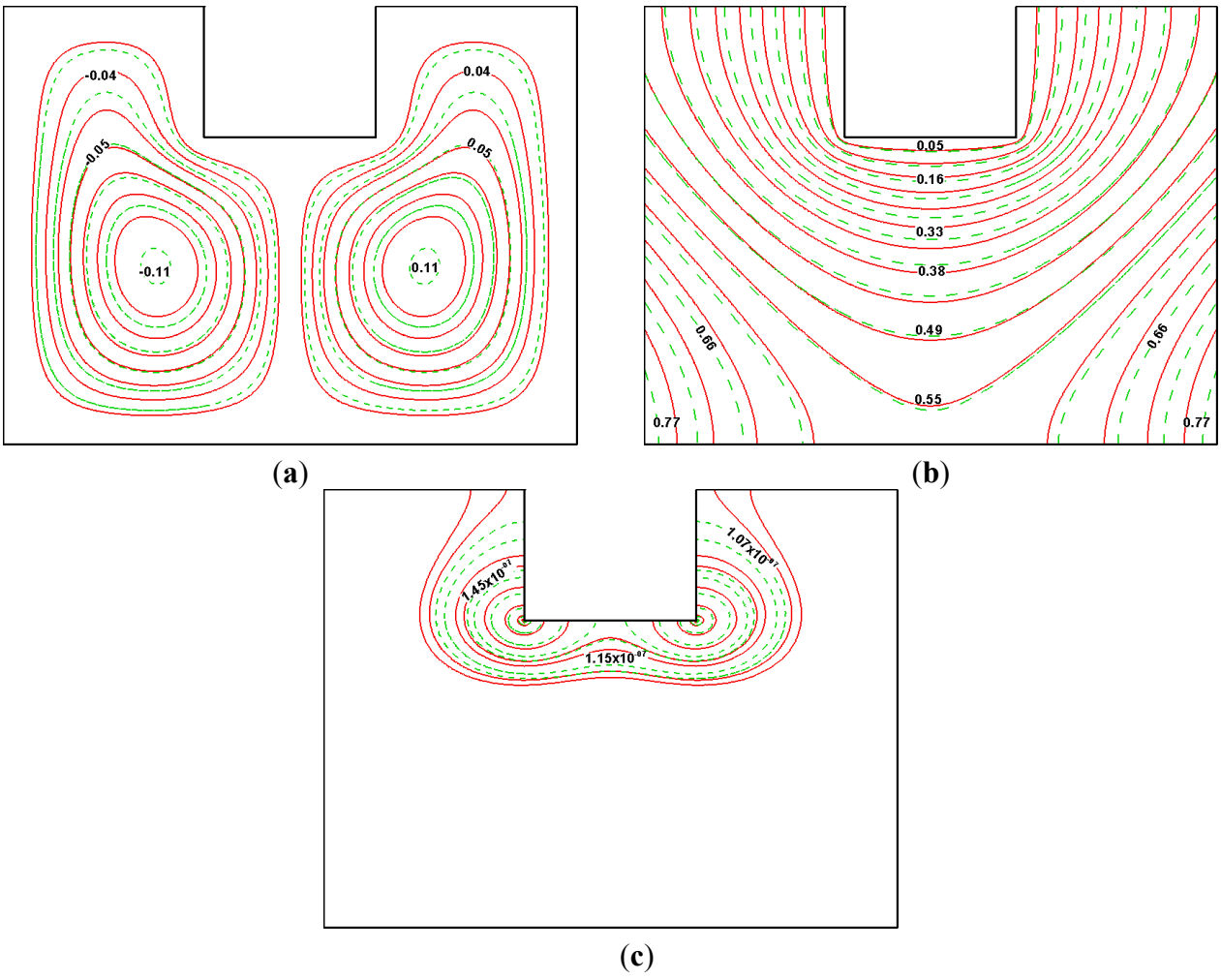

Figure 3. (**a**) Flow streamlines, (**b**) isotherms and (**c**) entropy generation given a Rayleigh number of $Ra = 10^3$. Note that solid line represents the pure water and dashed line represents nanofluid fluid with $\varphi = 4\%$. Note also that $W_L = 0.3W$, $H_L = 0.3W$ and $C_1 = 7.94 \times 10^{-10}$.

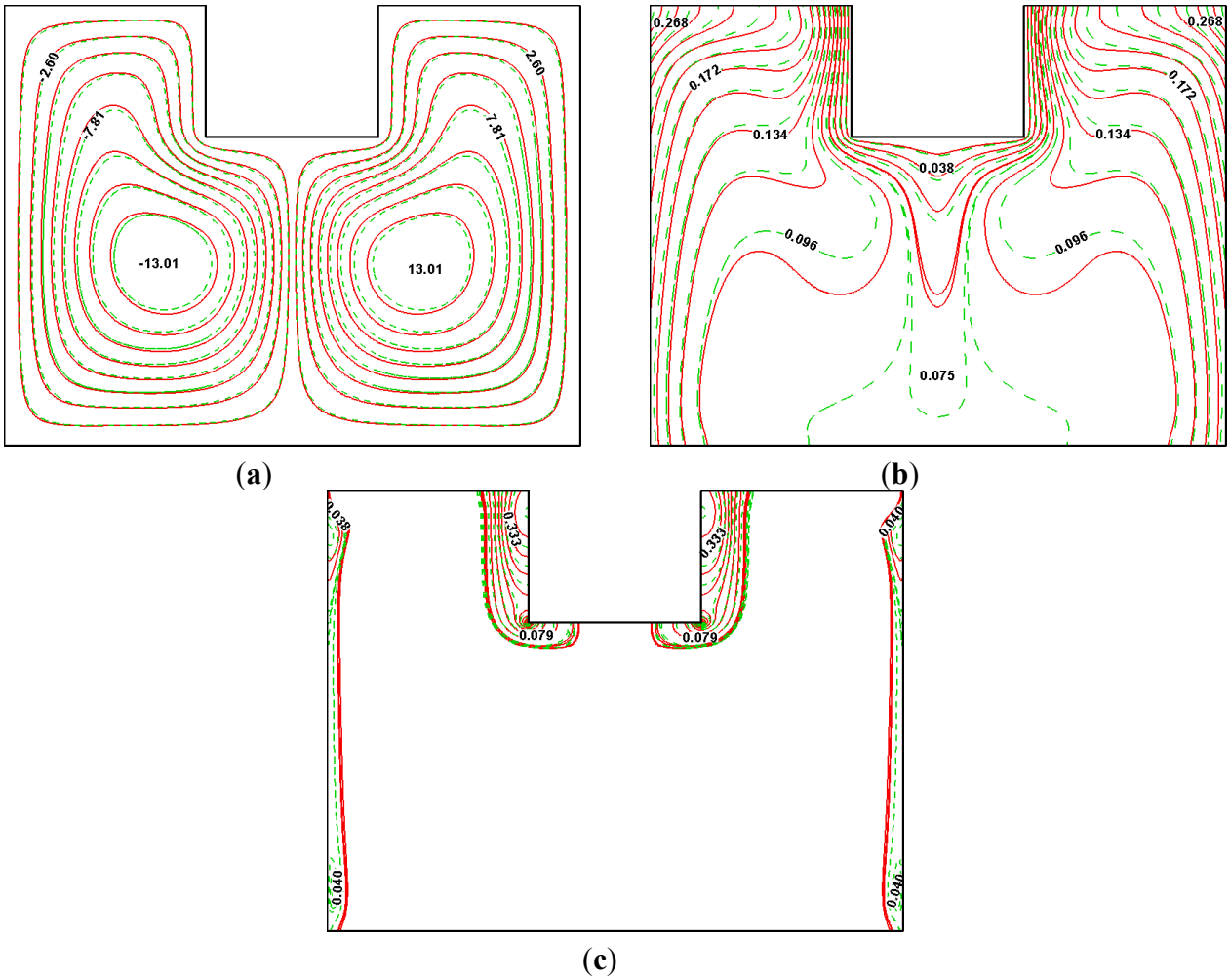

Figure 4. (**a**) Flow streamlines, (**b**) isotherms and (**c**) entropy generation given a Rayleigh number of $Ra = 10^6$. Note that solid line represents the pure water and dashed line represents nanofluid fluid with $\varphi = 4\%$. Note also that $W_L = 0.3W$, $H_L = 0.3W$ and $C_1 = 7.94 \times 10^{-10}$.

In addition, the addition of nanoparticles to the base fluid increases the thermal conductivity and viscosity of the working fluid. The increase of the viscosity decreases the fluid velocity. As a result, the strength of the streamlines is lower in the nanofluid than in pure water (see Figures 3a and 4a). The increase of the thermal conductivity in the nanofluid enhances the heat energy transport, leading to an improved heat transfer performance (see Figures 3b and 4b). Furthermore, since the Bejan number approaches unity for the two cases of Figures 3 and 4, the effect of the fluid friction irreversibility on the total entropy generation could be neglected. In other words, the heat transfer irreversibility dominates the total entropy generation. Since the addition of nanoparticles can increase the heat energy transport of the working fluid, the heat transfer irreversibility can be decreased. Consequently, the total entropy generation in nanofluid is lower than in pure fluid (see Figures 3c and 4c).

Figure 5 plots the variation of the local Nusselt number along the left heated wall for various nanoparticle volume fractions and Rayleigh numbers. Figure 6 shows the variations of the mean Nusselt number with the Rayleigh number as a function of the nanoparticle volume fraction. Given a low Rayleigh number, since the conduction mechanism dominates the heat transfer effect due to weak buoyancy effect, the local Nusselt number is low. Consequently, a low mean Nusselt number is obtained.

However, given a high Rayleigh number, the convection mechanism dominates the heat transfer and thus the fluid in the cavity is perturbed strongly by the convection mechanism. As a result, the local Nusselt number has a higher value and thus a higher mean Nusselt number is presented. In addition, since the addition of nanoparticles to the base fluid increases the thermal conductivity of the working fluid, the heat energy can be transported faster. As a result, nanofluid has a higher mean Nusselt number.

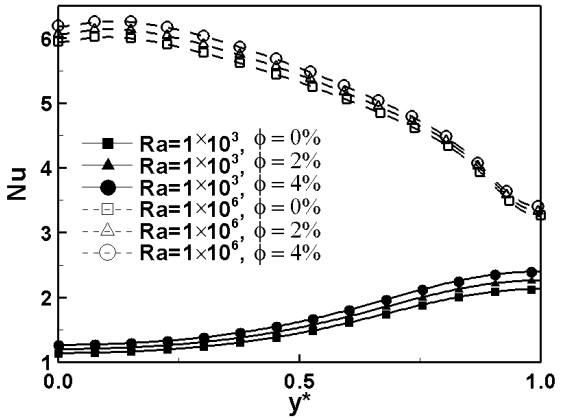

Figure 5. Variation of local Nusselt number along left heated wall for different nanoparticle volume fractions and Rayleigh numbers. Note that $W_L = 0.3W$ and $H_L = 0.3W$.

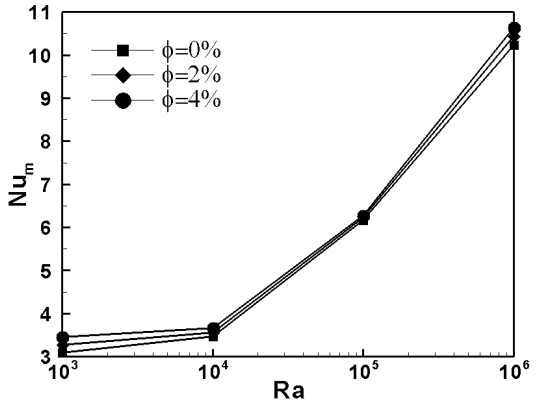

Figure 6. Variation of mean Nusselt number with Rayleigh number as function of nanoparticle volume fraction. Note that $W_L = 0.3W$ and $H_L = 0.3W$.

Figure 7 plots the variation of the total entropy generation with the Rayleigh number as a function of the nanoparticle volume fraction. Since the conduction mechanism dominates the heat transfer performance under the condition of a low Rayleigh number, the strength of the fluid flow is low and a low temperature gradient is presented. Therefore, the local entropy generations due to the fluid friction irreversibility and due to the heat transfer irreversibility are both low. Consequently, a low total entropy generation is obtained. However, given a high Rayleigh number, the heat transfer effect is dominated by the convection effect. Therefore, the strength of the fluid flow is high and a high temperature gradient is presented. As a result, the effects of fluid friction irreversibility and heat transfer irreversibility on the local entropy generation are increased. Consequently, the total entropy generation is higher. In addition, since the heat energy can be transported faster in nanofluid than in pure water, nanofluid has a lower total entropy generation.

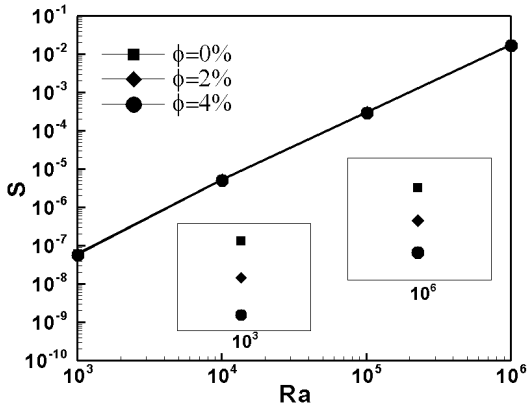

Figure 7. Variation of total entropy generation with Rayleigh number as function of nanoparticle volume fraction. Note that $W_L = 0.3W$, $H_L = 0.3W$, $C_1 = 7.94\times10^{-10}$ and $Be \approx 1.0$.

Figure 8 plots the variation of the Bejan number with the Eckert number as a function of the nanoparticle volume fraction. Generally, the magnitude of the viscous dissipation is determined by the Eckert number. Given the small value of the Eckert number, a low viscous dissipation is presented, resulting in a low fluid friction irreversibility. As a result, the effect of the fluid friction irreversibility on the total entropy generation can be ignored. Consequently, the heat transfer irreversibility dominates the total entropy generation, and thus the Bejan number approaches unity. As the Eckert number increases, the effect of the fluid friction irreversibility on the total entropy generation is increased. As a result, the Bejan number decreases. In addition, the thermal conductivity and viscosity of the working fluid both increases as the volume fraction of nanoparticle is increased. The two thermophysical properties have competing effects on the total entropy generation within the cavity. Since a low volume fraction of nanoparticle is added, the variation of the Bejan number is slight.

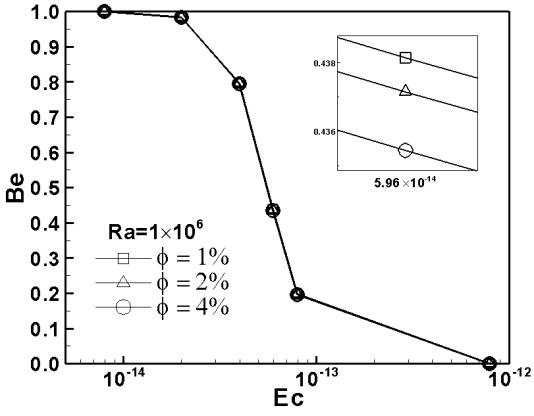

Figure 8. Variation of Bejan number with Eckert number as function of nanoparticle volume fraction given a Rayleigh number of $Ra = 10^6$. Note that $W_L = 0.3W$ and $H_L = 0.3W$.

Figure 9a,b show the variation of the mean Nusselt number and total entropy generation, respectively, with the geometry parameter W_L as a function of the Rayleigh number. As W_L increases, the distance between the low temperature walls and the heated walls shortens. As a result, the heat can be transported quickly from the heated walls to the low temperature walls. Therefore, in the range of

$W_L = 0.05W \sim W_L = 0.95W$, the mean Nusselt number increases as the width of W_L is increased. In addition, since the heat can be transported faster at a larger W_L, a low temperature gradient is presented in the cavity. Therefore, in the range of $W_L = 0.05W \sim W_L = 0.95W$, the total entropy generation decreases as the width of W_L is increased.

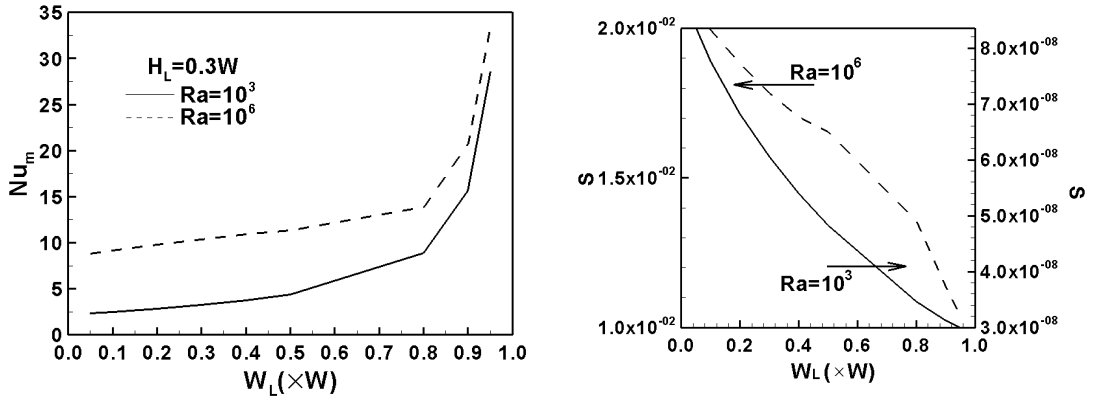

Figure 9. (**a**) Variation of mean Nusselt number with geometry parameter W_L as function of Rayleigh number, and (**b**) variation of total entropy generation with geometry parameter W_L as function of Rayleigh number. Note that $\varphi = 2\%$, $H_L = 0.3W$, $C_1 = 7.94 \times 10^{-10}$, and $Be \approx 1$.

Figure 10a,b shows the variation of the mean Nusselt number and total entropy generation, respectively, with the geometry parameter H_L as a function of the Rayleigh number. As H_L increases, the length of the low temperature walls lengthens. A larger heat transfer area is presented in the cavity, and thus the heat can be removed quickly. As a result, a higher mean Nusselt number and a lower total entropy generation are obtained.

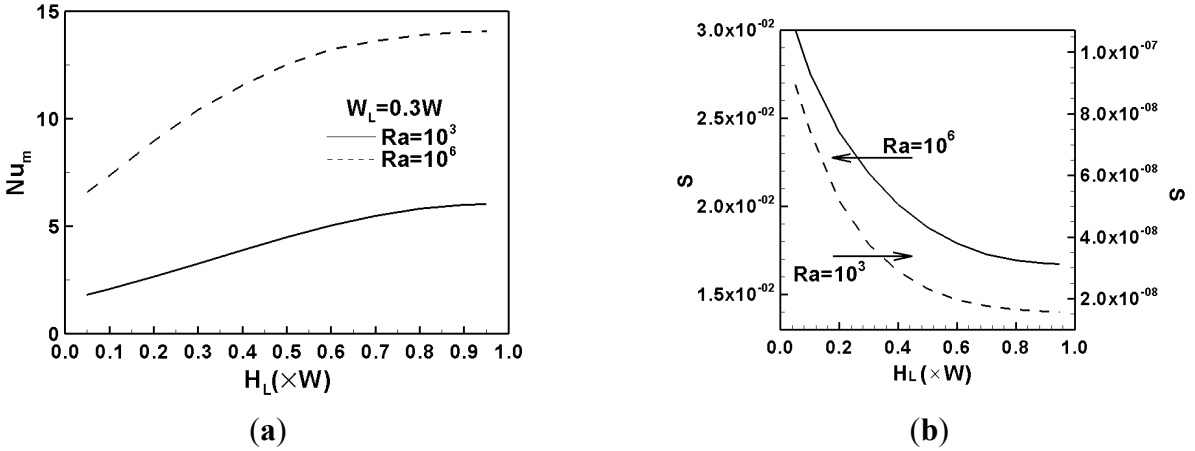

Figure 10. (**a**) Variation of mean Nusselt number with geometry parameter H_L as function of Rayleigh number, and (**b**) variation of total entropy generation with geometry parameter H_L as function of Rayleigh number. Note that $\varphi = 2\%$, $W_L = 0.3W$, $C_1 = 7.94 \times 10^{-10}$, and $Be \approx 1$.

Overall, the results presented in the study show that the mean Nusselt number can be increased and the total entropy generation can be reduced by widening the width of W_L extending the length of H_L, or increasing the volume fraction of nanoparticles. These results provide a useful source of reference for enhancing the heat transfer effect while simultaneously reducing the entropy generation.

4. Conclusions

This paper has studied the natural convection heat transfer performance and entropy generation in a U-shaped cavity filled with Al_2O_3-water nanofluid. In performing the study, the continuity equation, momentum equations, energy equation and Boussinesq approximation were used to govern the flow behavior and its heat transfer characteristics in the cavity, and the finite-volume method and SIMPLE C algorithm were utilized to solve the equations numerically. The effects of the nanoparticle volume fraction, the Rayleigh number and the geometry parameters on the mean Nusselt number and total entropy generation within the cavity were examined. The results have shown that as the volume fraction of the nanoparticle into the water increased, the mean Nusselt number was increased and total entropy generation was reduced. The results have also shown that as the Rayleigh number increased, the mean Nusselt number and the total entropy generation were both increased. It has been shown that given a constant Rayleigh number and nanoparticle volume fraction, the mean Nusselt number increased and the total entropy generation reduced by extending the length of the low temperature walls or widening the width of the low temperature walls.

Acknowledgments

The authors would like to thank the Ministry of Science and Technology, Taiwan, R.O.C. for the financial support of this study under Contract Nos. MOST 104-2221-E-167-001, MOST 104-2218-E-150-002 and MOST 104-2221-E-150-045.

Author Contributions

All authors have worked on this manuscript together and all authors have read and approved the final manuscript.

Conflicts of Interest

The authors declare no conflict of interest.

References and Notes

1. Bejan, A. Entropy generation through heat and fluid flow. *Int. J. Heat Mass Transf.* **1982**, *26*, 1728–1728.
2. Bejan, A. *Entropy Generation Minimization: The Method of Thermodynamic Optimization of Finite-Size Systems and Finite-Time Processes*; CRC Press: Boca Raton, FL, USA, 1996; pp. 1–400.
3. Ostrach, S. Natural convection in enclosures. *ASME J. Heat Transf.* **1988**, *110*, 1175–1190.

4. Erbay, L.B.; Altac, Z.; Sulus, B. An analysis of the entropy generation in a square enclosure. *Entropy* **2003**, *5*, 496–505.
5. Erbay, K.B.; Altac, Z.; Sulus, B. Entropy generation in a square enclosure with partial heating from a vertical lateral wall. *Heat Mass Transf.* **2004**, *40*, 909–918.
6. Magherbi, M.; Abbassi, H.; Brahim, A.B. Entropy generation at the onset of natural convection. *Int. J. Heat Mass Transf.* **2003**, *46*, 3441–3450.
7. Bouabid, M.; Magherbi, M.; Hidouri, N.; Brahim, A. B. Entropy generation at natural convection in an inclined rectangular cavity. *Entropy* **2011**, *13*, 1020–1033.
8. Ilis, G.G.; Mobedi, M.; Sunden, B. Effect of aspect ratio on entropy generation in a rectangular cavity with differentially heated vertical walls. *Int. Commun. Heat Mass Transf.* **2008**, *35*, 696–703.
9. Mukhopadhyay, A. Analysis of entropy generation due to natural convection in square enclosures with multiple discrete heat sources. *Int. Commun. Heat Mass Transf.* **2010**, *37*, 867–872.
10. Dagtekin, I.; Oztop, H.F.; Bahloul, A. Entropy generation for natural convection in Γ-shaped enclosures. *Int. Commun. Heat Mass Transf.* **2007**, *34*, 502–510.
11. Choi, S.U.S.; Eastman, J.A. Enhancing thermal conductivity of fluids with nanoparticles. International mechanical engineering congress and exhibition. *ASME-Publications-Fed* **1995**, *231*, 99–106.
12. Shahi, M.; Mahmoudi, A.H.; Raouf, A.H. Entropy generation due to natural convection cooling of a nanofluid. *Int. Commun. Heat Mass Transf.* **2011**, *38*, 972–983.
13. Kefayati, G.H.R. FDLBM simulation of entropy generation due to natural convection in an enclosure filled with non-Newtonian nanofluid. *Powder Technol.* **2015**, *273*, 176–190.
14. Parvin, S.; Chamkha, A.J. An analysis on free convection flow, heat transfer and entropy generation in an odd-shaped cavity filled with nanofluid. *Int. Commun. Heat Mass Transf.* **2014**, *54*, 8–17.
15. Cho, C.C.; Chen, C.L.; Chen, C.K. Natural convection heat transfer and entropy generation in wavy-wall enclosure containing water-based nanofluid. *Int. J. Heat Mass Transf.* **2013**, *61*, 749–758.
16. Cho, C.C. Heat transfer and entropy generation of natural convection in nanofluid-filled square cavity with partially-heated wavy surface. *Int. J. Heat Mass Transf.* **2014**, *77*, 818–827.
17. Ghasemi, B. Magnetohydrodynamic natural convection of nanofluids in U-shaped enclosures. *Numer. Heat Transf. Part A* **2013**, *63*, 473–487.
18. Cho, C.C.; Chen, C.L.; Chen, C.K. Natural convection heat transfer performance in complex-wavy wall enclosed cavity filled with nanofluid. *Int. J. Therm. Sci.* **2012**, *60*, 255–263.
19. Kefayati, G.H.R.; Hosseinizadeh, S.F.; Gorji, M.; Sajjadi, H. Lattice Boltzmann simulation of natural convection in tall enclosures using water/SiO_2 nanofluid. *Int. Commun. Heat Mass Transf.* **2011**, *38*, 798–805.
20. Kefayati, G.H.R.; Hosseinizadeh, S.F.; Gorji, M.; Sajjadi, H. Lattice Boltzmann simulation of natural convection an open enclosure subjugated to water/copper nanofluid. *Int. J. Therm. Sci.* **2012**, *52*, 91–101.
21. Patankar, S.V. *Numerical Heat Transfer and Fluid Flow*; McGraw-Hill: New York, NY, USA, 1980; pp. 1–197.
22. Davis, G.D.V. Natural convection of air in a square cavity a bench mark numerical solution. *Int. J. Numer. Methods Fluids* **1983**, *3*, 249–264.

23. Wan, D.C.; Patnaik, B.S.V.; Wei, G.W. A new benchmark quality solution for the buoyancy-driven cavity by discrete singular convolution. *Numer. Heat Transf. Part B* **2004**, *40*, 199–228.